

Effects of nitrogen flow rate on titanium nitride films deposition by DC facing target sputtering method

Hong Tak Kim, Jun Young Park, and Chinho Park[†]

School of Chemical Engineering, Yeungnam University, Gyeongsan 712-749, Korea

(Received 10 June 2011 • accepted 20 August 2011)

Abstract—TiN films were deposited onto a glass substrate by DC facing target sputtering, and the effects of N₂ flow rate on the film properties were investigated. Prepared TiN films had a rock salt (NaCl-type) structure with a very low resistivity (~30 μΩ·cm) and gold-like color. Increase in the N₂ flow rate played an important role in controlling the properties of TiN films, such as Ti/N ratio and growth orientation. The growth orientation changed from a (111) phase to (200), with the ratio of N/Ti becoming near stoichiometric. The change in the growth orientation was caused by the increase in the N₂ flow rate, which weakens the kinetic energy of the bombarding particles. The observed phenomenon is explained by an energy loss in the reactive plasma due to the difference in the inner degree of freedom of the molecular gas causing the reduction in the effective energy for radicals.

Key words: TiN, Facing Target Sputtering, FTS, Molecular Discharge, Texture Coefficient

INTRODUCTION

Titanium nitride (TiN) possesses outstanding properties, such as exceptional hardness, high thermal stability, high reflectance of infrared (IR) wavelengths, notable golden luster, high resistance to wear and corrosion, and good electrical conductivity [1-5]. As a result, TiN films have been used as the diffusion barriers and adhesive layers for electronic devices, tool hardening coatings, decorative coatings, heat mirrors, and solar cell applications [1-5].

Titanium nitride films have been largely deposited by chemical vapor and physical vapor deposition; these methods usually require a high reaction temperature to produce the final film with desired properties. Many problems exist for such high-temperature processes, including restriction of the kind of substrates to be used, unexpected phase transitions, and the difference in thermal expansion between the deposited material and substrate. Typically, plasma-enhanced processes are widely used to reduce the reaction temperature [2,6], but the samples could be damaged due to highly energetic ions in the plasma. Various modifications in the plasma enhanced processes were made to alleviate the damage, but the sample damage issue still remains to date. DC-facing target sputtering (FTS) is one of the most promising methods available for non-surface damage and low-growth temperature. These properties of FTS are useful towards deposition onto polymers or flexible substrates. Typically, a DC-FTS system consists of a couple of magnetron targets that are arranged oppositely, with the substrate placed on the outside of the targets. In this configuration, films can be deposited under high-density plasma without direct exposure of the energetic plasma.

In this study, TiN films were deposited onto a glass substrate using a DC-FTS at a relatively low temperature (~150°C), with the changes in film properties investigated as a function of the N₂ flow rate. The mechanisms behind the variation in the film properties are explained

in terms of discharge kinetics including molecular species.

EXPERIMENTAL DETAILS

The schematic diagram of the DC-facing target sputtering system for deposition of TiN films is shown in Fig. 1. The TiN films were deposited onto a soda-lime glass substrate using a gaseous mixture of argon and nitrogen. The distance between oppositely placed targets was 5 cm, and the distance between the substrate and the edge of two sputtering guns was 5 cm. The reaction chamber was evacuated by a mechanical pump and a turbo-molecular pump to the base pressure of 1.0×10^{-5} Torr. The working pressure was maintained at 4.0×10^{-3} Torr during film deposition, and the gas flow rate was controlled by a mass flow controller (KOFLOC 3660). The Ar flow rate was fixed at 40 sccm, with the N₂ flow rate ranging from 3 to 20 sccm. The pressure of the chamber was monitored with a capacitance manometer (MKS Baratron Type 122BA) and a Pen-

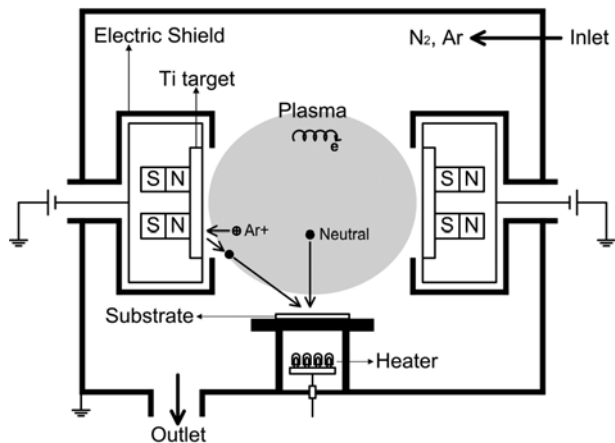


Fig. 1. Schematic diagram of the DC-facing target sputtering (DC-FTS) system for TiN film depositions.

[†]To whom correspondence should be addressed.

E-mail: chpark@ynu.ac.kr

nig gauge (Varian 525). The substrate temperature and applied power were fixed at 150 °C and 400 W, respectively. The film thickness and electrical resistivity of the prepared TiN films were measured by using a scanning electron microscope (SEM, Hitachi S-4200) and a 4-point probe system, respectively. The structural properties of the films were studied using an X-ray diffractometer (PANalytical X'Pert PRO). Optical properties such as TiN film reflectance and transmittance were investigated with a UV-Visible spectrophotometer (Varian CARY 5G), and the stoichiometric ratio of Ti/N was evaluated using an X-ray photo-spectrometer (VG Microtech, MT 500/1).

RESULTS AND DISCUSSION

The X-ray diffraction patterns (XRD) of the TiN films, as a function of N₂ flow rates, are shown in Fig. 2. As-grown TiN films had a rock salt (NaCl-type) structure, with (111), (200) and (220) peaks observed mainly at 2θ=36.8°, 42.8°, and 62.2° (JCPDS No. 38-1420). As the N₂ flow rate increased, the preferred orientation of the films changed from (111) plane to (200) plane. Especially, the degree of orientation for as-grown TiN films can be defined in terms of a texture coefficient (TC) [7-10], and the TC for (111) and (200) peaks, according to the N₂ flow rate, was calculated by the following equations:

$$TC(111) = \frac{I(111)}{I(111)+I(200)} \quad (1)$$

$$TC(200) = \frac{I(200)}{I(111)+I(200)} \quad (2)$$

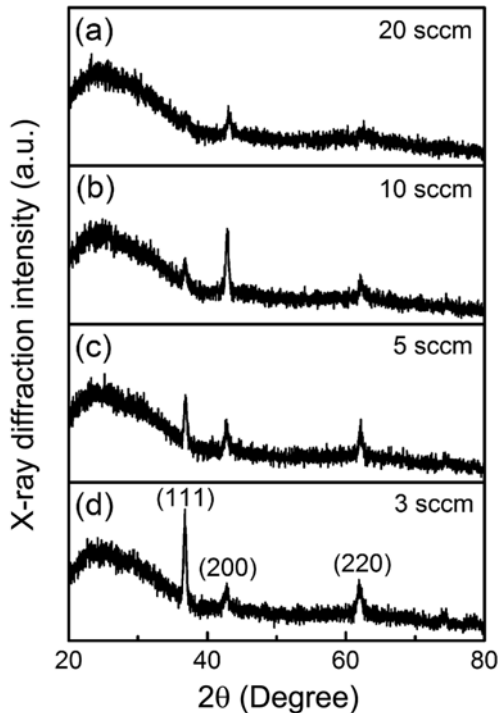


Fig. 2. X-ray diffraction patterns (XRD) of TiN films as a function of N₂ flow rate: (a) 20 sccm, (b) 10 sccm, (c) 5 sccm, (d) 3 sccm.

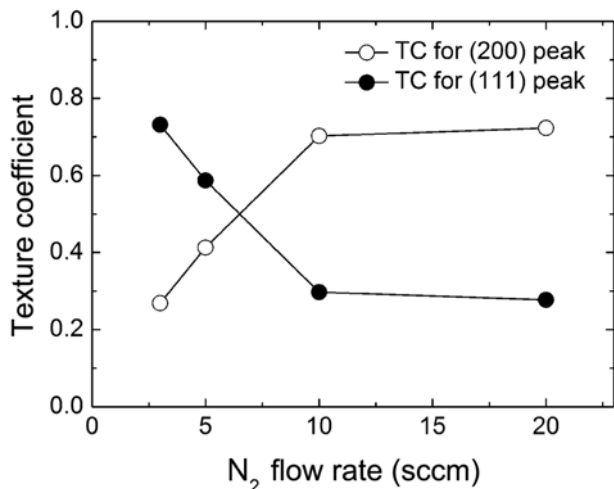


Fig. 3. Texture coefficient of (111) and (200) X-ray diffraction peak as a function of N₂ flow rate.

In the formulae above, I(111) and I(200) are the integrated intensity for the (111) and (200) XRD peaks, respectively.

Fig. 3 shows TC for (111) and (200) peaks as a function of the N₂ flow rate. The high value of the texture coefficient at a low N₂ flow rate indicates a highly preferred orientation towards (111) growth plane. The values of TC rapidly decrease when the N₂ flow rate increases to 10 sccm, while TC was saturated above the N₂ flow rate of 10 sccm. These changes in preferred orientations can be explained in terms of the energy of the bombarding particles onto the substrate. Generally, the incident particles on the substrate would be arranged to minimize the overall energy of the films during the deposition process, and are also strongly dependent upon film thickness [11-13]. The overall energy on the films is composed of the strain energy and the surface energy. The surface energy is dominant when the energy of the incident particles onto the substrate is relatively small, while strain energy is dominant when the energy of the incident particles onto the substrate is relatively high. In this study, molecular N₂ gas was used as the reactive gas to deposit TiN films, with the main distinctive feature between a molecular and atomic gas discharge being the inner molecular degree of freedom related to their vibrational and rotational motions. Experimental and theoretical results have shown that the main portion of the input energy in the molecular gas discharge is consumed for the excitation of the molecular vibrations [14-17]. These facts imply that the increase in the N₂ flow rate weakens the kinetic energy of the bombarding particles. Energy loss in the reactive plasma due to the change in the inner degree of freedom of molecular gas strongly affects not only the incident particles onto the target materials, but also the reactive particles in the plasma. Thus, the (200) preferred orientation was changed to a (111) orientation, as the kinetic energy of the bombarding particles on the substrate increased. This indicates that the kinetic energy of incident particles is an important factor in controlling the preferred orientation and crystallinity of the TiN films. Moreover, the film thickness was also one of the factors affecting the film growth orientation; the thickness of TiN films was kept constant in this study to get rid of any complexity involved with the effect of film thickness on growth orientation. Generally, the

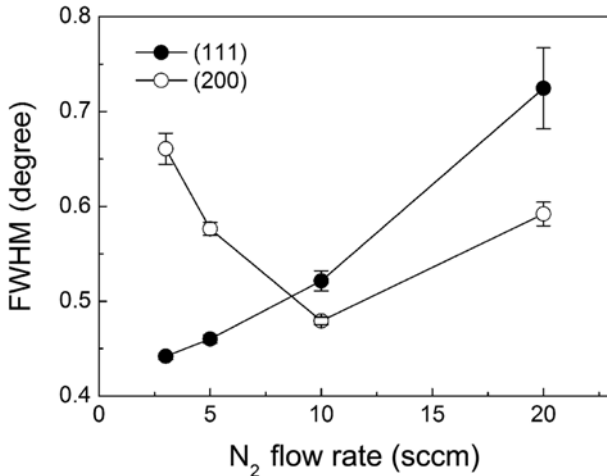


Fig. 4. Full width half maximum (FWHM) of (111) and (200) peaks according to N₂ flow rate.

effects of film thickness on growth orientation have been described as the strain energy becoming the dominant factor with film thickness increase, leading to the preferred orientation towards (111) plane in the TiN growth [11].

Fig. 4 shows the FWHM of the (111) and (200) peaks as a function of the N₂ flow rate. The FWHM of the (111) peaks increases with increasing N₂ flow rate. Otherwise, the FWHM of the (200) peaks decreases up to the N₂ flow rate of 10 sccm and then increases at higher N₂ flow rates. This tendency in the change of the (111) and (200) FWHM was similar to the change of TC's for (111) and (200) peak. The reason was explained by the results of competition between strain energy and surface energy. At a relatively high N₂ flow rate, it is speculated that incident particles falling onto the substrate do not possess sufficient energy to promote crystallization; thus, the films change gradually into an amorphous phase at the N₂ flow rate above 10 sccm.

Fig. 5 shows the nitrogen concentration on the TiN films according to the N₂ flow rates. The nitrogen concentration of the films de-

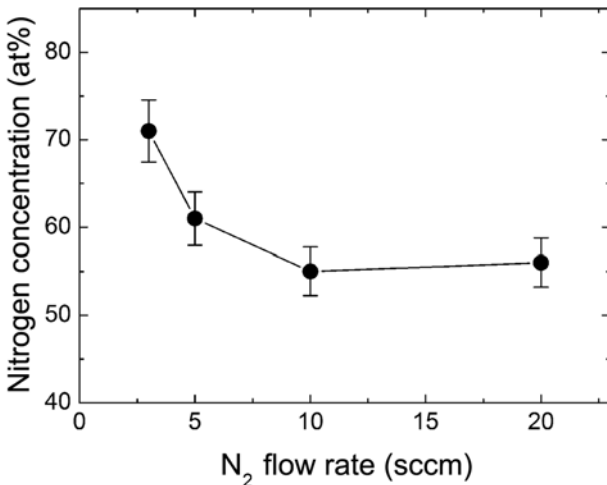


Fig. 5. Nitrogen concentration in TiN films as a function of N₂ flow rate.

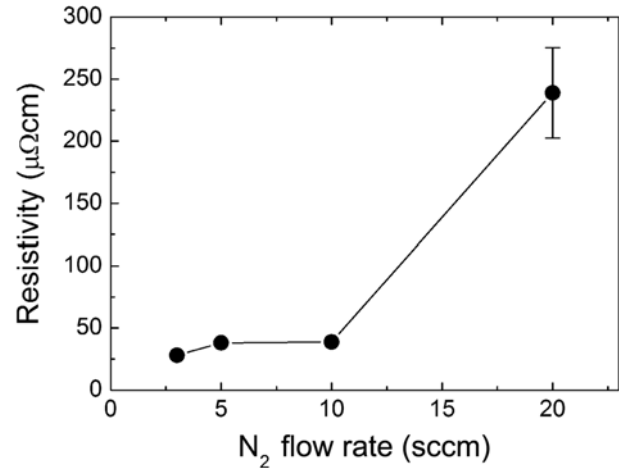


Fig. 6. Electrical resistivities of TiN films as a function of N₂ flow rate.

creases from 71 to 55 at% when the N₂ flow rate increases from 3 to 10 sccm, with the concentration saturated above the N₂ flow rate of 10 sccm. These results also suggest that the kinetic energy of reactive radicals is strongly related to the concentration of the nitrogen component of the films. As mentioned above, energy loss due to the change in the inner degree of freedom affects not only the incident particles onto the substrate, but also the reactive particles. This denotes that the energy distribution functions for the electrons and ions are strongly affected [6]. This leads to the overall decrease in the energetic radicals in the plasma when N₂ flow rate increases; these effects were regarded as the reason for the change in the nitrogen concentration within the TiN films.

Fig. 6 shows the electrical resistivity of the TiN films as a function of the N₂ flow rate. The resistivity of the TiN films increases slightly from 28.0 $\mu\Omega\text{cm}$, at a N₂ flow rate of 3 sccm, to 38.8 $\mu\Omega\text{cm}$ at 10 sccm of N₂. However, the resistivity of the films shows a sudden increase above the N₂ flow rate of 10 sccm. Many factors, such as deviations from the stoichiometric ratio of Ti/N, crystallinity, grain size, and incorporation of impurities, are known to affect the TiN film resistivity [1,2,18]. In this study, effects of crystallinity on the films are considered to play an important role in changing the film resistivity. As mentioned in the XRD results, the crystallinity of TiN films above the 10 sccm of N₂ gradually degrades and changes into amorphous phase. Thus, crystallinity is considered to be the primary factor in increasing the resistivity of the films in this study.

Fig. 7 shows the reflectance and transmittance spectra of TiN films at a N₂ flow rate of 3 (dashed line) and 10 sccm (solid line), respectively. The reflectance spectra of all TiN films are exhibited by a strong absorption in the blue wavelength region with the reflectance minimum near 450 nm, a steep edge in a visible wavelength, and mirror like properties in an IR region. These optical properties of the TiN films can be explained in terms of partial densities of the d-state and an atomic selection rule [1-3,19].

The reflectance of TiN films increases when the N₂ flow rate increases from 3 to 10 sccm. As mentioned above, the nitrogen concentration in the films decreased with an increasing N₂ flow rate, thus implying that the optical properties of the TiN films are closely

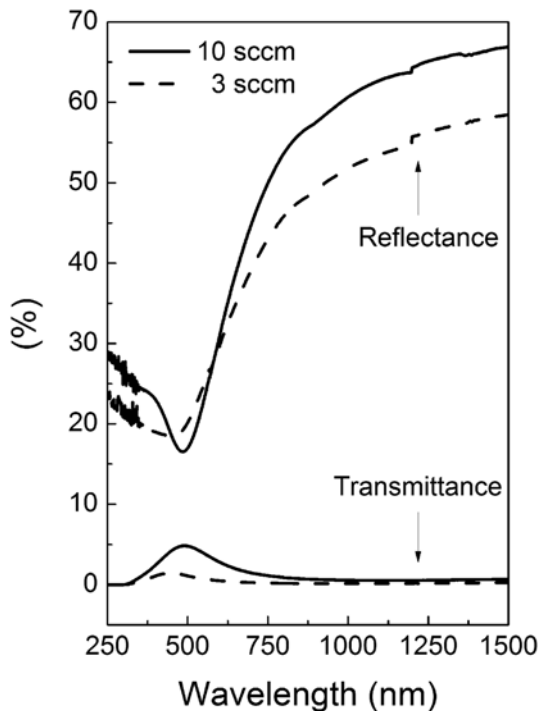


Fig. 7. Reflectance and transmittance spectra of TiN films at different N_2 flow rates: 3 sccm (dashed line) and 10 sccm (solid line).

related to the N_2 concentration in the films. In addition, the reflectance of the films was strongly related to the number of free electrons in the films and the rise of the number of free electrons caused the increase in the reflectance of the TiN films [3]. Furthermore, the ionic bonding model can account for the free electrons that moved from the nitrogen site to form the bond between Ti and N. Thus, an increase in the N concentration leads to a decrease in the number of free electrons, causing the corresponding decrease in TiN film reflectance.

CONCLUSIONS

TiN films were deposited onto glass substrates by the DC-FTS method, and the effects of N_2 flow rate on the film properties were investigated systematically. TiN film depositions were carried out at a relatively low temperature (150°C), and prepared TiN films exhibited a gold-like color, very low resistivity ($\sim 30 \mu\Omega\cdot\text{cm}$), and a rock salt structure. As the N_2 flow rate increased, the preferred orientation of the films changed from a (111) to a (200) plane. The change in the growth orientation, due to the competition between the surface and strain energies in the films, was strongly related to the kinetic energy of incident particles onto the substrate, and the

N_2 flow rate mainly affected the kinetic energy loss due to change in the inner degree of freedom of molecular gases. The DC-FTS can be slated as one of the promising methods to deposit TiN films onto flexible substrates due to its relatively lower deposition temperature with the capability of producing good film qualities.

ACKNOWLEDGEMENTS

This work was supported by the 2008 Yeungnam University research grant (208-A-251-076), and the Human Resources Development Program of the Korea Institute of Energy Technology Evaluation and Planning (KETEP) grant (No. 20104010100580), funded by the Korean Ministry of Knowledge Economy.

REFERENCES

1. J. E. Sundgren, *Thin Solid Films*, **128**, 21 (1985).
2. H. T. Kim, C. S. Chae, D. H. Han and D. K. Park, *J. Korean Phys. Soc.*, **37**, 319 (2000).
3. S. Niyomsoan, W. Grant, D. L. Olson and B. Mishra, *Thin Solid Films*, **415**, 187 (2002).
4. B. J. Yoo, K. J. Kim, Y. H. Kim, K. K. Kim, M. J. Ko, W. M. Kim and N. G. Park, *J. Mater. Chem.*, **21** 3077 (2011).
5. G. Hyett, R. Binions and I. P. Parkin, *Chem. Vapor Deposition*, **13**, 675 (2007).
6. M. A. Lieberman and A. J. Lichtenberg, *Principles of plasma discharges and materials processing*, John Wiley & Sons Inc., Toronto (1994).
7. W. J. Chou, G. P. Yu and J. H. Huang, *Surf. Coat. Technol.*, **149**, 7 (2002).
8. C. Barret and T. B. Massalski, *Structure of Metals*, Pergamon, Oxford (1980).
9. J. A. Montes de Oca Valero, Y. Le Petitcorps, J. P. Manaud, G. Cholalon, F. J. Carrillo Romo and A. Lopez M., *J. Vac. Sci. Technol. A*, **23**(3), 394 (2005).
10. S. H. Kim, H. Park, K. H. Lee, S. H. Jee, D. J. Kim, Y. S. Yoon and H. B. Chae, *J. Ceram. Process. Res.*, **10**(1), 49 (2009).
11. U. C. Oh and J. H. Je, *J. Appl. Phys.*, **74**, 1692 (1993).
12. E. Penilla and J. Wang, *J. Nanomaterials*, doi:10.1155/2008/267161.
13. J. P. Zhao, X. Wang, T. S. Shi and X. H. Liu, *J. Appl. Phys.*, **79**(12), 9399 (1996).
14. A. V. Eletskii and B. M. Smirnov, *Physics Uspekhi*, **39**(11), 1137 (1996).
15. V. Yu. Baranov and K. N. Zh Ul'yanov, *Tekh. Fiz.*, **39**, 249 (1969).
16. K. N. Ul'yanov, *Tekh. Fiz.*, **43**, 570 (1971).
17. H. T. Kim and D. K. Park, *J. Korean Phys. Soc.*, **42**, S916 (2003).
18. N. Y. Kim, Y. B. Son, J. H. Oh, C. K. Hwangbo and M. C. Park, *Surf. and Coat. Technol.*, **128-129**, 156 (2000).
19. A. R. Forouhi and I. Bloomer, *Phys. Rev. B*, **38**, 1865 (1988).